

**Analysis of Intrinsic Stability Criteria for Isotropic
Third-Order Green Elastic and Compressible
Neo-Hookean Solids**

by John. D. Clayton and Karen M. Bliss

ARL-RP-475

March 2014

A reprint from *Mechanics of Materials*, Vol. 68, pp. 104–119, 2014.

NOTICES

Disclaimers

The findings in this report are not to be construed as an official Department of the Army position unless so designated by other authorized documents.

Citation of manufacturer's or trade names does not constitute an official endorsement or approval of the use thereof.

Destroy this report when it is no longer needed. Do not return it to the originator.

Army Research Laboratory

Aberdeen Proving Ground, MD 21005-5066

ARL-RP-475

March 2014

Analysis of Intrinsic Stability Criteria for Isotropic Third-Order Green Elastic and Compressible Neo-Hookean Solids

John. D. Clayton

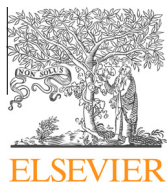
Weapons and Materials Research Directorate, ARL

Karen M. Bliss

United States Military Academy

A reprint from *Mechanics of Materials*, Vol. 68, pp. 104–119, 2014.

REPORT DOCUMENTATION PAGE			<i>Form Approved</i> OMB No. 0704-0188		
Public reporting burden for this collection of information is estimated to average 1 hour per response, including the time for reviewing instructions, searching existing data sources, gathering and maintaining the data needed, and completing and reviewing the collection information. Send comments regarding this burden estimate or any other aspect of this collection of information, including suggestions for reducing the burden, to Department of Defense, Washington Headquarters Services, Directorate for Information Operations and Reports (0704-0188), 1215 Jefferson Davis Highway, Suite 1204, Arlington, VA 22202-4302. Respondents should be aware that notwithstanding any other provision of law, no person shall be subject to any penalty for failing to comply with a collection of information if it does not display a currently valid OMB control number. PLEASE DO NOT RETURN YOUR FORM TO THE ABOVE ADDRESS.					
1. REPORT DATE (DD-MM-YYYY) March 2014		2. REPORT TYPE Reprint		3. DATES COVERED (From - To) January 2012–January 2014	
4. TITLE AND SUBTITLE Analysis of Intrinsic Stability Criteria for Isotropic Third-Order Green Elastic and Compressible Neo-Hookean Solids			5a. CONTRACT NUMBER		
			5b. GRANT NUMBER		
			5c. PROGRAM ELEMENT NUMBER		
6. AUTHOR(S) John. D. Clayton and Karen M. Bliss*			5d. PROJECT NUMBER AH80		
			5e. TASK NUMBER		
			5f. WORK UNIT NUMBER		
7. PERFORMING ORGANIZATION NAME(S) AND ADDRESS(ES) U.S. Army Research Laboratory ATTN: RDRL-WMP-C Aberdeen Proving Ground, MD 21005-5066			8. PERFORMING ORGANIZATION REPORT NUMBER ARL-RP-475		
9. SPONSORING/MONITORING AGENCY NAME(S) AND ADDRESS(ES)			10. SPONSOR/MONITOR'S ACRONYM(S)		
			11. SPONSOR/MONITOR'S REPORT NUMBER(S)		
12. DISTRIBUTION/AVAILABILITY STATEMENT Approved for public release; distribution is unlimited. * Department of Mathematical Sciences, United States Military Academy, West Point, NY 10996					
13. SUPPLEMENTARY NOTES A reprint from <i>Mechanics of Materials</i> , Vol. 68, pp. 104–119, 2014.					
14. ABSTRACT Internal stability of isotropic nonlinear elastic materials under homogeneous deformation is studied. Results provide new insight into various intrinsic stability measures, first proposed elsewhere, for generic nonlinear elastic solids. Three intrinsic stability criteria involving three different tangent elastic stiffness matrices are considered, corresponding to respective increments in strain measures conjugate to thermodynamic tension, first Piola–Kirchhoff stress, and Cauchy stress. Primary deformation paths of interest include spherical (i.e., isotropic) deformation, uniaxial strain, and simple shear; unstable modes are not constrained to remain along primary deformation paths. Effects of choices of second- and third-order elastic constants on intrinsic stability are systematically studied for physically realistic ranges of constants. For most cases investigated here, internal stability according to strain increments conjugate to Cauchy stress is found to be the most stringent criterion. When third-order constants vanish, internal stability under large compression tends to decrease as Poisson’s ratio increases. When third-order constants are nonzero, a negative (positive) pressure derivative of the shear modulus often promotes unstable modes in compression (tension). For large shear deformation, larger magnitudes of third-order constants tend to result in more unstable behavior, regardless of the sign of the pressure derivative of the shear modulus. A compressible neo-Hookean model is generally much more intrinsically stable than second- and third-order elastic models when Poisson’s ratio is non-negative.					
15. SUBJECT TERMS nonlinear elasticity, stability, third-order elastic constants, isotropy, polycrystals					
16. SECURITY CLASSIFICATION OF:			17. LIMITATION OF ABSTRACT	18. NUMBER OF PAGES	19a. NAME OF RESPONSIBLE PERSON John. D. Clayton
a. REPORT Unclassified	b. ABSTRACT Unclassified	c. THIS PAGE Unclassified			UU



Analysis of intrinsic stability criteria for isotropic third-order Green elastic and compressible neo-Hookean solids



J.D. Clayton ^{a,*}, K.M. Bliss ^b

^a Impact Physics, RDRL-WMP-C, US Army Research Laboratory, Aberdeen Proving Ground, MD 21005-5066, USA

^b Department of Mathematical Sciences, US Military Academy – West Point, NY 10996, USA

ARTICLE INFO

Article history:

Received 5 June 2012

Received in revised form 8 August 2013

Available online 23 August 2013

Keywords:

Nonlinear elasticity

Internal stability

Third-order elastic constants

Isotropy

Polycrystals

ABSTRACT

Internal stability of isotropic nonlinear elastic materials under homogeneous deformation is studied. Results provide new insight into various intrinsic stability measures, first proposed elsewhere, for generic nonlinear elastic solids. Three intrinsic stability criteria involving three different tangent elastic stiffness matrices are considered, corresponding to respective increments in strain measures conjugate to thermodynamic tension, first Piola–Kirchhoff stress, and Cauchy stress. Primary deformation paths of interest include spherical (i.e., isotropic) deformation, uniaxial strain, and simple shear; unstable modes are not constrained to remain along primary deformation paths. Effects of choices of second- and third-order elastic constants on intrinsic stability are systematically studied for physically realistic ranges of constants. For most cases investigated here, internal stability according to strain increments conjugate to Cauchy stress is found to be the most stringent criterion. When third-order constants vanish, internal stability under large compression tends to decrease as Poisson's ratio increases. When third-order constants are nonzero, a negative (positive) pressure derivative of the shear modulus often promotes unstable modes in compression (tension). For large shear deformation, larger magnitudes of third-order constants tend to result in more unstable behavior, regardless of the sign of the pressure derivative of the shear modulus. A compressible neo-Hookean model is generally much more intrinsically stable than second- and third-order elastic models when Poisson's ratio is non-negative.

Published by Elsevier Ltd.

1. Introduction

Stability of elastic solids under finite deformation has been the subject of numerous studies, with early work on intrinsic stability of crystals due to Born (1940). Nonlinear elastic anisotropic solids (e.g., single crystals) have been analyzed in a number of works (Hill, 1975; Hill and Milstein, 1977; Milstein and Hill, 1979; Wang et al., 1993, 1995; Morris and Krenn, 2000), as have nonlinear elastic isotropic solids (Hill, 1957; Rivlin, 1974; Rivlin and Beatty, 2003).

Various criteria for stability of elastic solids have been proposed in the literature, beginning with work of Born

(1940) who associated stability with a positive definite stiffness measure and local convexity of internal energy expressed in terms of a Lagrangian Green strain measure. In a real physical system, the appropriate choice of stability criterion depends on the method of static incremental load application (e.g., dead loading in one or more directions (Rivlin, 1974)) and any constraints associated with boundary conditions, and such a criterion may not correspond to Born's. When considering “intrinsic” or “internal” stability of a unit cell or unit cube of a given material, from the continuum viewpoint or using atomic theory, the proper choice of stability measure is ambiguous when the precise loading mechanism is left unspecified. Different choices of conjugate stress–strain measures (i.e., different generalized coordinates and conjugate forces) can lead to different

* Corresponding author. Tel.: +1 4102786146.

E-mail address: john.d.clayton1.civ@mail.mil (J.D. Clayton).

local convexity conditions and different intrinsic stability criteria (Hill, 1975; Hill and Milstein, 1977). As stated by Milstein and Hill (1979), consistency of classical, unique, and environment-dependent stability criteria with intrinsic stability or convexity arguments such as Born's requires a special environment in which loads can be varied to follow the material during any disturbances while fixing values of conjugate forces, which in turn are non-unique since they depend on the choice of generalized coordinates (i.e., the choice of strain measure). This load environment used to probe stability (e.g., via virtual deformations at a fixed stress) need not correspond to the loading program used to achieve the stressed equilibrium state from which stability is tested (Hill and Milstein, 1977; Milstein and Hill, 1979).

Intrinsic stability requirements considered in the present work lead to restrictions on various incremental tangent elastic moduli; stability measures of this sort applied to superposed deformation variations in any direction may require that an energy function be locally convex, or at least that a particular stiffness matrix (i.e., Hessian) be positive definite, at the current equilibrium state. For nonlinear materials of high symmetry (e.g., isotropic solids) under simple deformation paths, such intrinsic stability requirements can often be stated succinctly in terms of restrictions on a few strain-dependent elastic coefficients. In linear elastic solids, such requirements degenerate to the usual constitutive constraints of positive bulk and shear moduli. As noted above and explained in Hill and Milstein (1977) and Parry (1978), intrinsic stability measures like those considered herein do not depend on the load environment, but do depend on the choice of conjugate stress–strain measures. Comparisons among intrinsic criteria involving different Lagrangian strain measures were derived for generic isotropic elastic solids under positive principal stresses (Parry, 1978).

The distinction between material instability and structural instability should be noted. As defined in the present work, material instability correlates with intrinsic instability, and depends only on material properties and loading protocol. Intrinsic stability criteria are local since they consider only homogeneous stress/deformation states up to the onset of instability. In nonlinear materials (e.g., nonlinear elastic, elastic–plastic, or damaged solids), the onset of material instability depends on strain, but in linear elastic solids, material stability is independent of strain and simply requires positive definiteness of the tensor of elastic constants. In contrast, structural instability criteria are global rather than local, depending on geometry of the body. The stress/strain state may be inhomogeneous prior to onset of structural instability. Structural instability may occur even if the material is intrinsically stable, and can be induced by loads even in linear elastic materials. A representative example is buckling of a slender column under compression.

Intrinsic stability properties of solids under large compressive stress or pressure are of interest for applications in ballistics, impact phenomena, and earth and planetary sciences. Elastic instability may signal the onset of failure or localization phenomena, e.g., slip, fracture, or phase transformations (Hill, 1975; Wang et al., 1993; Morris

and Krenn, 2000). Hard materials of lower symmetry such as quartz (Gregoryanz et al., 2000), silicon carbide (Clayton, 2010), and boron carbide (Clayton, 2012) exhibit a decrease in certain shear elastic stiffness components with increasing pressure. At high pressures, this tendency may lead to the onset of instability and subsequent amorphization (Chen et al., 2003), which in the case of ceramic materials hinders performance in ballistic applications. In contrast to these polyatomic ceramic materials, most elemental engineering materials demonstrate increasing shear moduli with increasing pressure (Guinan and Steinberg, 1974), which would tend to enhance rather than diminish internal stability at large compressions.

Nonlinear elastic models of anisotropic single crystals (Wallace, 1972; Teodosiu, 1982; Clayton, 2011) typically assume a strain energy function written as a Taylor polynomial in Green (Lagrangian) elastic strain $\mathbf{E} = \frac{1}{2}(\mathbf{F}^T\mathbf{F} - \mathbf{1})$, with \mathbf{F} the deformation gradient. Such a model, when terms of up to third order are maintained (i.e., second- and third-order elastic constants) provides reasonably accurate descriptions of stresses and wave propagation for moderate compressions (Thurston, 1974; Clayton, 2009); however, Eulerian strain measures may be more accurate for extreme pressures (Weaver, 1976; Jeanloz, 1989).

The present work focuses primarily on isotropic elastic solids of third order. Such materials are described by two independent second-order elastic constants and three independent third-order elastic constants (Murnaghan, 1937; Teodosiu, 1982). Because of the limited number of constants, systematic study of effects of choices of constants on intrinsic stability for simple monotonic deformation paths is tractable, and is undertaken in this work. Third-order constants are related explicitly to pressure derivatives of bulk and shear moduli in the reference state (Thurston et al., 1966; Guinan and Steinberg, 1974; Teodosiu, 1982); experimental data (Guinan and Steinberg, 1974; Steinberg, 1982) thus provide realistic bounds on combinations of third-order constants. Choices of third-order constants yielding a decreasing shear stiffness with increasing compression provide insight into behavior of aforementioned ceramic materials demonstrating shear instabilities at high pressure (Gregoryanz et al., 2000; Chen et al., 2003). It is noted that single crystals of such materials are highly anisotropic (e.g., trigonal symmetry: six second-order and fourteen third-order elastic constants) and systematic study of effects of varying all elastic constants individually on stability is intractable. For comparison, intrinsic stability of a class of compressible neo-Hookean solids (Simo and Pister, 1984), which demonstrate a strongly increasing bulk modulus with pressure, is also considered.

This paper is organized as follows. Requisite quantities associated with internal stability are derived in Section 2. Intrinsic stability of third-order elastic solids in terms of three different criteria from the literature (Born, 1940; Hill, 1975; Wang et al., 1993) is analyzed in Section 3. For each criterion, minimum eigenvalues of a particular tangent stiffness matrix are examined for different choices of second- and/or third-order elastic constants for an element of material undergoing spherical deformation, uniaxial

strain, and simple shear. Implicitly assumed in this analysis are availability of so-called “passive” loading environments (Hill and Milstein, 1977; Milstein and Hill, 1979) that make possible application of any of the three criteria mentioned already, permitting unstable modes in any strain direction that may or may not be coaxial with the imposed primary deformation path up to the checkpoint for instability. Complementary analysis of such internal stability of neo-Hookean solids is also undertaken. Although some general constraints have been derived elsewhere for cubic crystals under pressure (Wang et al., 1993) and neo-Hookean solids under dead loading (Rivlin, 1974; Rivlin and Beatty, 2003), effects of ranges of elastic constants on all of the considered intrinsic stability criteria for either of these two kinds of material models have not, to the authors’ knowledge, been reported elsewhere.

Notational conventions of continuum mechanics are used. Vectors and higher-order tensors are written in bold italics, scalars and scalar components in italics. Stiffness tensors and matrices are written in serif fonts (e.g., \mathbf{A} , \mathbf{B} , etc.) All are referred to a fixed Cartesian frame, with referential components in capitals and spatial components in lower-case. Greek indices are used for Voigt notation. Summation applies over repeated indices.

2. Nonlinear elasticity and intrinsic stability measures

2.1. General theory

Let \mathbf{x} and \mathbf{X} denote spatial and reference coordinates. The deformation gradient is the invertible two-point tensor

$$\mathbf{F} = \partial\mathbf{x}/\partial\mathbf{X}, \quad F_{ij} = \partial x_i / \partial X_j, \quad (2.1)$$

where $i, j = 1, 2, 3$. By the polar decomposition theorem,

$$\mathbf{F} = \mathbf{R}\mathbf{U}, \quad \mathbf{R}^{-1} = \mathbf{R}^T, \quad \mathbf{U} = \mathbf{U}^T, \quad (2.2)$$

where \mathbf{U} is positive definite. The Jacobian determinant giving the ratio of current to initial volume is

$$J = \det\mathbf{F} = \det\mathbf{U} > 0. \quad (2.3)$$

The Green (Lagrangian) strain tensor and deformation tensor are

$$\mathbf{E} = \frac{1}{2}(\mathbf{C} - \mathbf{1}), \quad E_{IJ} = \frac{1}{2}(C_{IJ} - \delta_{IJ}); \quad (2.4)$$

$$\mathbf{C} = \mathbf{F}^T\mathbf{F} = \mathbf{U}^2, \quad C_{IJ} = F_{kl}F_{kj} = U_{IK}U_{JK}. \quad (2.5)$$

Cauchy stress $\boldsymbol{\sigma} = \boldsymbol{\sigma}^T$, first Piola–Kirchhoff stress \mathbf{P} , and second Piola–Kirchhoff stress (i.e., thermodynamic tension) $\mathbf{S} = \mathbf{S}^T$ are related by

$$\boldsymbol{\sigma} = J^{-1}\mathbf{P}\mathbf{F}^T = J^{-1}\mathbf{F}\mathbf{S}\mathbf{F}^T, \quad \sigma_{ij} = J^{-1}P_{iK}F_{jK} \\ = J^{-1}F_{iL}S_{LK}F_{jK}. \quad (2.6)$$

Cauchy pressure is $p = -\frac{1}{3}\sigma_{ii}$.

For a hyperelastic material with properties independent of \mathbf{X} , strain energy per unit reference volume W is of the general form

$$W = W[\mathbf{C}(\mathbf{F})] = W[\mathbf{E}(\mathbf{F})] = W(\mathbf{F}). \quad (2.7)$$

Stresses are

$$\mathbf{P} = \frac{\partial W}{\partial \mathbf{F}} = 2\mathbf{F} \frac{\partial W}{\partial \mathbf{C}} = \mathbf{F} \frac{\partial W}{\partial \mathbf{E}} = \mathbf{F}\mathbf{S}. \quad (2.8)$$

Second-order tangent elastic moduli are

$$\mathbf{A}(\mathbf{F}) = \frac{\partial \mathbf{P}}{\partial \mathbf{F}} = \frac{\partial^2 W}{\partial \mathbf{F} \partial \mathbf{F}}, \quad \mathbf{C}(\mathbf{E}) = \frac{\partial \mathbf{S}}{\partial \mathbf{E}} = \frac{\partial^2 W}{\partial \mathbf{E} \partial \mathbf{E}} = 4 \frac{\partial^2 W}{\partial \mathbf{C} \partial \mathbf{C}}. \quad (2.9)$$

These are related by Simo and Pister (1984) and Clayton (2011) as

$$A_{ijkl} = F_{ii}F_{kk}C_{ijkl} + S_{jL}\delta_{ik} \quad (2.10)$$

and possess the symmetry properties

$$A_{ijkl} = A_{klij}, \quad C_{ijkl} = C_{klij} = C_{jilk} = C_{iljk}. \quad (2.11)$$

Three intrinsic or internal stability criteria, all frequently encountered in various solid mechanics, physics, or materials science literature, are addressed in what follows. First, consider stability with respect to allowable variations, from a possibly stressed equilibrium state, in Green strain, $\delta\mathbf{E}$. The following internal stability criterion (also denoting local convexity) is usually attributed to Born (1940):

$$\delta\mathbf{S} \cdot \delta\mathbf{E} = \delta\mathbf{E} \cdot \mathbf{C} \cdot \delta\mathbf{E} = \delta E_\alpha C_{\alpha\beta} \delta E_\beta > 0, \quad (2.12)$$

where $[C_{\alpha\beta}]$ is the symmetric 6×6 matrix corresponding to \mathbf{C} in Voigt notation ($\alpha, \beta = 1, 2, \dots, 6$). The actual net potential energy change (internal work to second order minus virtual work at fixed \mathbf{S}) is half the quantity on the left side of inequality (2.12) in the context of a trapezoidal rule for quadrature (Hill, 1975); inclusion or omission of a factor of $\frac{1}{2}$ does not change the stability criterion. A necessary and sufficient condition for (2.12) to hold under arbitrary non-zero $\delta\mathbf{E}$ is

$$\det[C_{\alpha\beta}] > 0. \quad (2.13)$$

At instability, $[C_{\alpha\beta}]$ has null or negative eigenvalue(s), with corresponding eigenmodes δE_α . When the current configuration is taken as reference,

$$c_{ijkl}(\mathbf{F}) = J^{-1}F_{ii}F_{jj}F_{kk}F_{ll}C_{ijkl}, \quad \delta e_{ij} = F_{ki}^{-1}F_{lj}^{-1}\delta E_{kl} \quad (2.14)$$

and since $J > 0$, criterion (2.12) and (2.13) is equivalent to

$$\delta E_{ij}C_{ijkl}\delta E_{kl} = J\delta e_{ij}c_{ijkl}\delta e_{kl} > 0 \iff \det[c_{\alpha\beta}] > 0. \quad (2.15)$$

Nonzero eigenvalues of \mathbf{c} and \mathbf{C} may be different, but the critical deformation \mathbf{F}^* at which either first exhibits a zero eigenvalue is the same. Criteria (2.12) and (2.15) are equivalent to Eqs. (4.1)–(4.3) of Hill (1975). Although early calculations (Born, 1940; Misra, 1940) focused on unstressed lattices, this criteria has often been posited for stressed materials.

A second internal stability criterion can be expressed as the inequality (Hill, 1957, 1975)

$$\delta\mathbf{P} \cdot \delta\mathbf{F} = \delta\mathbf{F} \cdot \mathbf{A} \cdot \delta\mathbf{F} > 0, \quad (2.16)$$

where $\delta\mathbf{F}$ is an admissible variation in deformation gradient. Criterion (2.16) is equivalent to Eq. 4.20 of Hill (1975) applied in the context of dead loading. For cases in which variations are restricted to strain only, $\delta\mathbf{F} \rightarrow \delta\mathbf{U} = (\delta\mathbf{U})^T$, and (2.16) reduces to, considering all possible strain increments,

$$\delta \mathbf{U} \cdot \mathbf{A} \cdot \delta \mathbf{U} = \delta U_{\alpha} A_{\alpha\beta} \delta U_{\beta} > 0 \iff \det[A_{\alpha\beta}] > 0, \quad (2.17)$$

where $[A_{\alpha\beta}]$ is the symmetric 6×6 matrix corresponding to

$$A_{ijkl} = \frac{1}{4} (A_{ijkl} \delta_{ii} \delta_{kk} + A_{jikl} \delta_{jj} \delta_{kk} + A_{ijlk} \delta_{ii} \delta_{ll} + A_{jilk} \delta_{jj} \delta_{ll}). \quad (2.18)$$

When the current configuration is taken as reference,

$$a_{ijkl}(\mathbf{F}) = J^{-1} F_{jj} F_{ll} A_{ijkl}, \quad \delta e_{ij} = \frac{1}{2} (F_{ki}^{-1} \delta F_{jk} + F_{kj}^{-1} \delta F_{ik}) \quad (2.19)$$

and since $J > 0$, criterion (2.17) can also be expressed as

$$\delta U_{ij} A_{ijkl} \delta U_{kl} = J \delta e_{ij} a_{ijkl} \delta e_{kl} > 0 \iff \det[a_{\alpha\beta}] > 0. \quad (2.20)$$

As noted in Clayton (2012), this is equivalent to the so-called GCN⁺ condition, listed as constitutive inequality (8A.21) of Wang and Truesdell (1973).

A third intrinsic stability criterion is (Wang et al., 1993; Morris and Krenn, 2000)

$$\delta \boldsymbol{\sigma} \cdot \delta \mathbf{e} = \delta \mathbf{e} \cdot \mathbf{B} \cdot \delta \mathbf{e} > 0, \quad (2.21)$$

where $\delta \mathbf{e}$ is a nonzero strain increment defined by

$$\delta \mathbf{e} = \mathbf{F}^{-T} \delta \mathbf{E} \mathbf{F}^{-1}, \quad \delta e_{ij} = F_{ki}^{-1} \delta E_{kl} F_{lj}^{-1} \quad (2.22)$$

and work conjugate to Cauchy stress since

$$\delta W = \mathbf{S} \cdot \delta \mathbf{E} = \mathbf{P} \cdot \delta \mathbf{F} = \mathbf{J} \boldsymbol{\sigma} \cdot \delta \mathbf{e}. \quad (2.23)$$

Incremental tangent modulus giving change in Cauchy stress with respect to strain is (Wallace, 1972; Wang et al., 1993; Morris and Krenn, 2000; Clayton, 2012)

$$B_{ijkl} = c_{ijkl} + \frac{1}{2} (\sigma_{ik} \delta_{jl} + \sigma_{il} \delta_{jk} + \sigma_{jk} \delta_{il} + \sigma_{jl} \delta_{ik} - \sigma_{ij} \delta_{kl} - \sigma_{kl} \delta_{ij}). \quad (2.24)$$

Tensor \mathbf{B} in (2.24) exhibits full Voigt symmetry:

$$B_{ijkl} = B_{klij} = B_{jikl} = B_{ijlk}. \quad (2.25)$$

Correspondingly, denoting $[B_{\alpha\beta}]$ the symmetric 6×6 form of \mathbf{B} , internal stability holds with respect to Cauchy stress if and only if

$$\det[B_{\alpha\beta}] > 0. \quad (2.26)$$

Condition (2.21) is identical to Eq. (30) of Morris and Krenn (2000), and the corresponding instability criterion is identical to Eq. (2.26) of Wang et al. (1995). Symmetrized tangent stiffness \mathbf{B} is identical in the current work and these other works (Wang et al., 1993; Wang et al., 1995; Morris and Krenn, 2000; Clayton, 2012); notation used in Wang et al. (1993) and Wang et al. (1995) for “Lagrangian” strain corresponds to an increment in Lagrangian strain measured with respect to a stressed reference state and is identical to (2.22) of the present work, as derived explicitly by Wallace (1967). A criterion similar to (2.21) was declared to be in accord with the “exact” condition for classical stability of hydrostatically loaded cubic crystals with moduli dictated by pairwise atomic interactions (Milstein and Hill, 1979).

Although the first equality in (2.21) does not strictly apply for cases in which rotation of the material $\mathbf{R} \neq \mathbf{1}$, condition (2.26) has been interpreted (Morris and Krenn, 2000) as a necessary, but not always sufficient, intrinsic

stability criterion for arbitrary (i.e., unconstrained) load increments. Utility of criteria incorporating variations in rotation such as (2.16) with $\delta \mathbf{F} \neq (\delta \mathbf{F})^T$ as conditions for the onset of structural changes in materials is questionable, since even the zero stress state is a boundary point of the (un)stable domain when rotations arise (Hill, 1975). Noting that under rotations of the spatial frame, $\delta \mathbf{e}$ transforms objectively (similarly to the symmetric deformation rate tensor) but $\delta \boldsymbol{\sigma}$ generally does not, the leftmost side of (2.21) is not necessarily objective with respect to changes among rotating spatial frames of reference. This deficiency in the B stability criterion has apparently not been emphasized in prior works that employ it (Wang et al., 1993; Wang et al., 1995; Morris and Krenn, 2000), and no attempt is made to address it further here. When $\delta \boldsymbol{\sigma} = -\delta p \mathbf{1}$ is a pressure increment, objectivity of (2.21) does hold. Furthermore, term $\delta \mathbf{e} \cdot \mathbf{B} \cdot \delta \mathbf{e}$ following the equality in (2.21), and hence criterion (2.26), is invariant under change of spatial basis since \mathbf{B} transforms like a fourth-order tensor.

Minimum eigenvalues of symmetric 6×6 matrix forms of \mathbf{C} , \mathbf{A} , and \mathbf{B} are labeled Λ_C , Λ_A , and Λ_B . Since in the undeformed and stress free reference state $\mathbf{C} = \mathbf{A} = \mathbf{B}$, the minimum eigenvalue of all of these matrices in said reference state is denoted Λ_0 .

Considered later in Section 3 are homogeneous deformations of a volume element (e.g., a unit cube) of uniform material. Each of the C, A, and B intrinsic stability criteria is treated as equally plausible since the particular means by which incremental traction is applied to such a volume under virtual deformations from the homogeneously deformed state is left unspecified. For a specific situation involving dead loading, for which traction per unit reference area and hence \mathbf{P} is held fixed during stretch variation \mathbf{U} , the A criterion (2.17) would be most appropriate. When the loading mechanism fixes the Cauchy stress, e.g., as in conventional hydrostatic compression or tension (Milstein and Hill, 1979; Wang et al., 1993; Wang et al., 1995), then B criterion (2.21) would be most appropriate, as discussed in Milstein and Hill (1979) and Morris and Krenn (2000). The C criterion (2.12) does not correlate readily with any real load control mechanism (since there is no traction vector associated with \mathbf{S} that is independent of deformation), but is considered in this paper because of its historical significance (Born, 1940; Misra, 1940; Hill, 1975) and widespread use in physics and materials science (Gregoryanz et al., 2000). Viewed another way, a comparison of convexity criteria as generalized coordinates (i.e., strain measures) vary is analogous to a comparison of classical elastic stability criteria as the load environment varies (Parry, 1978).

Consideration of finite strain and correct work conjugate stress–strain measures is essential for meaningful study of deformation-induced material instability. These different measures enter the C, A, and B criteria defined above. In contrast, in linear elasticity theory, different stress tensors (\mathbf{S} , \mathbf{P} , $\boldsymbol{\sigma}$) and strain tensors (\mathbf{E} , \mathbf{U} , \mathbf{e}) become indistinguishable, and intrinsic stability does not depend on strain since tangent stiffness is constant; e.g., for an isotropic linear elastic solid the local stability requirement degenerates to (3.5).

2.2. Third-order elasticity

Strain energy density written as a Taylor series in Green strain \mathbf{E} is

$$\begin{aligned} W &= W^0 + C_{IJ}^0 E_{IJ} + \frac{1}{2!} C_{IJKL}^0 E_{IJ} E_{KL} + \frac{1}{3!} C_{IJKLMN}^0 E_{IJ} E_{KL} E_{MN} + \dots \\ &= W^0 + \left. \frac{\partial U}{\partial E_{IJ}} \right|_{\mathbf{E}=0} E_{IJ} + \left. \frac{1}{2} \frac{\partial^2 U}{\partial E_{IJ} \partial E_{KL}} \right|_{\mathbf{E}=0} E_{IJ} E_{KL} \\ &\quad + \left. \frac{1}{6} \frac{\partial^3 U}{\partial E_{IJ} \partial E_{KL} \partial E_{MN}} \right|_{\mathbf{E}=0} E_{IJ} E_{KL} E_{MN} + \dots \end{aligned} \quad (2.27)$$

Vanishing energy and stress in the undeformed reference state leads to $W^0 = 0$ and $C_{IJ}^0 = 0$, and henceforth restricting attention to third-order elasticity,

$$\begin{aligned} W &= \frac{1}{2} C_{IJKL}^0 E_{IJ} E_{KL} + \frac{1}{6} C_{IJKLMN}^0 E_{IJ} E_{KL} E_{MN} \\ &= \frac{1}{2} C_{\alpha\beta}^0 E_\alpha E_\beta + \frac{1}{6} C_{\alpha\beta\gamma}^0 E_\alpha E_\beta E_\gamma. \end{aligned} \quad (2.28)$$

Stress \mathbf{S} and tangent modulus \mathbf{C} are

$$S_\alpha = C_{\alpha\beta}^0 E_\beta + \frac{1}{2} C_{\alpha\beta\gamma}^0 E_\beta E_\gamma, \quad C_{\alpha\beta} = C_{\alpha\beta}^0 + C_{\alpha\beta\gamma}^0 E_\gamma. \quad (2.29)$$

Second- and third-order constants in Voigt notation are $C_{\alpha\beta}^0$ and $C_{\alpha\beta\gamma}^0$. For homogeneous isotropic materials, elastic constant tensors are of the form [Teodosiu \(1982\)](#)

$$C_{IJKL}^0 = \lambda(\delta_{IJ}\delta_{KL}) + G(\delta_{IK}\delta_{JL} + \delta_{IL}\delta_{JK}), \quad (2.30)$$

$$\begin{aligned} C_{IJKLMN}^0 &= \alpha[\delta_{IJ}\delta_{KL}\delta_{MN}] + \beta[\delta_{IJ}(\delta_{KM}\delta_{LN} + \delta_{KN}\delta_{LM}) \\ &\quad + \delta_{KL}(\delta_{IM}\delta_{JN} + \delta_{IN}\delta_{JM}) + \delta_{MN}(\delta_{IK}\delta_{JL} + \delta_{IL}\delta_{JK})] \\ &\quad + \chi[\delta_{IK}(\delta_{JM}\delta_{LN} + \delta_{JN}\delta_{LM}) + \delta_{JL}(\delta_{IM}\delta_{KN} + \delta_{IN}\delta_{KM}) \\ &\quad + \delta_{IL}(\delta_{JM}\delta_{KN} + \delta_{JN}\delta_{KM}) + \delta_{JK}(\delta_{IM}\delta_{LN} + \delta_{IN}\delta_{LM})]. \end{aligned} \quad (2.31)$$

The theory of third-order elastic isotropic solids with five independent elastic constants was developed by [Murnaghan \(1937\)](#). Second-order elastic constants obey the familiar relations

$$\begin{aligned} \lambda &= C_{12}^0, \quad G = C_{44}^0 = \frac{1}{2}(C_{11}^0 - C_{12}^0), \quad K \\ &= \lambda + \frac{2}{3}G, \quad \nu = \frac{\lambda}{2(\lambda + G)}, \end{aligned} \quad (2.32)$$

where G, K , and ν are shear modulus, bulk modulus, and Poisson's ratio in the reference state. Third-order elastic constants obey

$$\begin{aligned} \alpha &= C_{123}^0, \quad \beta = C_{144}^0 = \frac{1}{2}(C_{112}^0 - C_{123}^0), \quad \chi = C_{456}^0 \\ &= \frac{1}{8}(C_{111}^0 - 3C_{112}^0 + 2C_{123}^0). \end{aligned} \quad (2.33)$$

Second-order compliance components $M_{\alpha\beta}^0 = [C_{\alpha\beta}^0]^{-1}$ are

$$\begin{aligned} M_{11}^0 &= \frac{C_{11}^0 + C_{12}^0}{(C_{11}^0 - C_{12}^0)(C_{11}^0 + 2C_{12}^0)}, \\ M_{12}^0 &= \frac{-C_{12}^0}{(C_{11}^0 - C_{12}^0)(C_{11}^0 + 2C_{12}^0)}; \end{aligned} \quad (2.34)$$

it follows that $M_{44}^0 = 2(M_{11}^0 - M_{12}^0) = 1/C_{44}^0 = 1/G$. Derivatives of second-order moduli $C_{\alpha\beta}$ with respect to pressure are, at the undeformed reference state (i.e., $F = \mathbf{1} \Rightarrow E = 0$),

$$C'_{\alpha\beta} = \left. \frac{\partial C_{\alpha\beta}}{\partial p} \right|_{F=\mathbf{1}}, \quad (2.35)$$

where in full tensor notation ([Thurston et al., 1966](#)),

$$C'_{IJKL} = \left. \frac{\partial C_{IJKL}}{\partial E_{MN}} \frac{\partial E_{MN}}{\partial S_{PQ}} \frac{\partial S_{PQ}}{\partial p} \right|_{F=\mathbf{1}} = -C_{IJKLMN}^0 M_{MNPQ}^0. \quad (2.36)$$

For third-order isotropic materials,

$$\begin{aligned} C'_{11} &= -\frac{1}{3K}(C_{111}^0 + 2C_{112}^0), \\ C'_{12} &= -\frac{1}{3K}(2C_{112}^0 + C_{123}^0), \end{aligned} \quad (2.37)$$

leading to pressure derivatives of thermodynamic bulk and shear moduli at the reference state:

$$\begin{aligned} K' &= -\frac{1}{9K}(C_{111}^0 + 6C_{112}^0 + 2C_{123}^0), \quad G' \\ &= -\frac{1}{6K}(C_{111}^0 - C_{123}^0). \end{aligned} \quad (2.38)$$

Conditions for which stiffness tensor \mathbf{C} remains isotropic under finite deformation have been recently discussed ([Fuller and Brannon, 2011](#)). Full Cauchy symmetry ([Clayton, 2011](#)) corresponds to $\lambda = G$ and $\alpha = \beta = \chi$.

2.3. Neo-Hookean elasticity

For a compressible neo-Hookean material, strain energy density is

$$\begin{aligned} W &= W^0 + \frac{1}{2}G(\text{trC} - 3) + f(J) \\ &= W^0 + \frac{1}{2}G(F_{ii}F_{ii} - 3) + f(J), \end{aligned} \quad (2.39)$$

where function f accounts for compressibility. For the particular kind of neo-Hookean solid considered here, which demonstrates vanishing stress and energy in the reference state ([Simo and Pister, 1984](#)),

$$W = \frac{1}{2}G(\text{trC} - 3) - G \ln J + \frac{1}{2}\lambda(\ln J)^2. \quad (2.40)$$

Noting that $\partial \ln J / \partial C = \frac{1}{2}C^{-1}$, stress \mathbf{S} and tangent modulus \mathbf{C} are

$$S_{IJ} = 2 \frac{\partial W}{\partial C_{IJ}} = G\delta_{IJ} + (\lambda \ln J - G)C_{IJ}^{-1}, \quad (2.41)$$

$$\begin{aligned} C_{IJKL} &= 4 \frac{\partial^2 W}{\partial C_{IJ} \partial C_{KL}} \\ &= \lambda C_{IJ}^{-1} C_{KL}^{-1} + (G - \lambda \ln J)(C_{IK}^{-1} C_{JL}^{-1} + C_{IL}^{-1} C_{JK}^{-1}). \end{aligned} \quad (2.42)$$

In the reference state, $C^{-1} = \mathbf{1}$, $J = 1$, and (2.30) and (2.42) are consistent; relations among second-order constants for neo-Hookean elasticity obey (2.32). Considering spherical deformation of the form $C_{ij} = J^{2/3} \delta_{ij}$ such that $\sigma_{ij} = -p\delta_{ij}$, pressure derivatives of bulk and shear moduli at the reference state are

$$\begin{aligned}
 K' &= \frac{\lambda}{K} \left[2 + \frac{8}{9} \left(\frac{1}{2\nu} - 1 \right) \right], \\
 G' &= \frac{\lambda}{K} \left[1 + \frac{4}{3} \left(\frac{1}{2\nu} - 1 \right) \right].
 \end{aligned}
 \tag{2.43}$$

Extension of this neo-Hookean model to elastic–plastic materials and expressed in general curvilinear coordinates can be found elsewhere (Clayton, 2012).

3. Intrinsic stability under particular deformation paths

Homogeneous deformations of an element of isotropic material are considered. Minimum eigenvalue ratios Λ_C/Λ_0 , Λ_A/Λ_0 , and Λ_B/Λ_0 are compared for fully imposed spherical, uniaxial, and shearing paths, recalling that a zero eigenvalue corresponds to the onset of intrinsic instability, e.g., loss of local convexity associated with a given stiffness tensor for the current deformed state. Eigenvalues and corresponding orthonormal eigenvectors (i.e., eigenmodes) are computed numerically as the deformation is incremented along each path. Eigenmodes are not restricted to align with the primary (imposed) deformation path; when critical modes do not, then possibility of bifurcation from the primary path is implied.

At the conclusion of each applied increment of deformation, it is assumed that a (possibly fictitious) loading apparatus is available enabling virtual variations in strain (δE , δU , or δe) in any direction while holding the conjugate stress measure (S, P , or σ , respectively) fixed (Hill, 1975; Hill and Milstein, 1977). Such conditions enable formal application of the intrinsic stability criteria defined in Section 2.1. A similar approach was taken in Clayton (2012) in a study of internal stability of a particular material of lower symmetry (boron carbide ceramic), where following (Wang et al., 1995), internal stability was referred to as “mechanical stability”.

3.1. Imposed deformation paths

Prescribed deformation is parameterized as follows in terms of a single scalar ε , letting $\{e_1, e_2, e_3\}$ denote an orthonormal basis. Spherical (and hence hydrostatic stress states for isotropic materials):

$$\mathbf{F} = \mathbf{U} = (1 + \varepsilon)^{1/3} \mathbf{1}, \quad J = 1 + \varepsilon;
 \tag{3.1}$$

Uniaxial strain along e_1 :

$$\mathbf{F} = \mathbf{U} = \mathbf{1} + \varepsilon e_1 \otimes e_1, \quad J = 1 + \varepsilon;
 \tag{3.2}$$

Simple shear in the $e_1 - e_2$ plane:

$$\mathbf{F} = \mathbf{RU} = \mathbf{1} + \varepsilon e_1 \otimes e_2, \quad J = 1;
 \tag{3.3}$$

$$[F_{ij}] = [R_{ik}][U_{kj}] = \begin{bmatrix} \frac{2}{(4+\varepsilon^2)^{1/2}} & \frac{\varepsilon}{(4+\varepsilon^2)^{1/2}} & 0 \\ \frac{-\varepsilon}{(4+\varepsilon^2)^{1/2}} & \frac{2}{(4+\varepsilon^2)^{1/2}} & 0 \\ 0 & 0 & 1 \end{bmatrix} \begin{bmatrix} \frac{2}{(4+\varepsilon^2)^{1/2}} & \frac{\varepsilon}{(4+\varepsilon^2)^{1/2}} & 0 \\ \frac{\varepsilon}{(4+\varepsilon^2)^{1/2}} & \frac{2+\varepsilon^2}{(4+\varepsilon^2)^{1/2}} & 0 \\ 0 & 0 & 1 \end{bmatrix}.
 \tag{3.4}$$

Effects of various values of elastic constants on internal stability under the above deformation paths are computed

and analyzed for respective Green elastic and compressible neo-Hookean solids in Section 3.2 and Section 3.3.

3.2. Green elasticity

Considered first are materials for which all third-order elastic constants vanish, i.e., St. Venant–Kirchhoff solids. In this case, $C_{ijkl} = C_{jkl}^0 = \text{constant}$, and internal stability constraints in the unstressed and undeformed reference state are

$$\det[C_{\alpha\beta}] > 0 \iff \Lambda_0 = \Lambda_C > 0 \iff K > 0 \text{ and } G > 0.
 \tag{3.5}$$

These can also be associated with local strain energy convexity at the reference state. The rightmost conditions in (3.5) imply $-1 < \nu < \frac{1}{2}$. Noting that $G = \lambda(\frac{1}{2\nu} - 1)$, at a given value of ν , energy W , stresses, and tangent elastic coefficients are all proportional to λ . Hence Λ_A/Λ_0 and Λ_B/Λ_0 depend only on ν and ε for a particular deformation path. Ratio $\Lambda_C/\Lambda_0 = 1$ regardless of ν and ε and is of no interest. Considered in Fig. 1 are results for $-1 < \nu < \frac{1}{2}$. Intrinsic instability occurs as $\Lambda/\Lambda_0 \rightarrow 0$, i.e., as a curve intersects the horizontal axis of each figure.

As shown in Fig. 1(a) and (b) for spherical deformation, as ν increases, stability in tension ($\varepsilon > 0$) increases, and in compression ($\varepsilon < 0$) decreases. The B stability criterion of (2.26) tends to be more stringent than the A criterion of (2.17), i.e., a zero eigenvalue is more often attained at a smaller magnitude of ε for the former, particularly for $\nu \geq 0$. As shown in Fig. 1(c) and 1(d) for uniaxial strain, if $\nu \leq 0$ then instability may occur in both tension and compression. As shown in Fig. 1(e) and (f) for simple shear, stability increases with increasing ν , with Λ_A/Λ_0 and Λ_B/Λ_0 remaining positive for $\nu \geq 0$ and $\varepsilon \leq 0.8$. The B criterion provides a more stringent measure of stability than the A criterion for shear deformation. As discussed more in the Appendix, as the material tends towards incompressibility ($\nu \rightarrow 0.5$), intrinsic stability declines rapidly under spherical or uniaxial compression.

Even though third-order constants are zero for results shown in Fig. 1, the theory is still geometrically nonlinear and mathematically valid at large magnitudes of finite strain parameter ε , i.e., results shown do not correspond to classical linear elasticity theory, which does not distinguish among Piola–Kirchhoff and Cauchy stresses, for example. Vanishing third-order constants corresponds to $K' = G' = 0$ in (2.38), which as will be noted later, is an exceptional case that does not hold for most elemental polycrystalline solids. Results in Fig. 1 are important, however, because St. Venant–Kirchhoff theory is widely used, especially in the context of finite elastic–plastic theories of metal plasticity (Rashid and Nemat-Nasser, 1992; Clayton and McDowell, 2004; Clayton, 2006). Results also provide a basis of comparison for calculations reported next wherein stiffness \mathbf{C} is not constant.

Considered next are cases for which one or more third-order constants (i.e., α, β, χ or $C_{111}^0, C_{112}^0, C_{123}^0$) may be non-zero. Attention is focused on ranges of values physically realistic for polycrystalline engineering materials (e.g., metals, ceramics, and minerals). Ultrasonic measurements

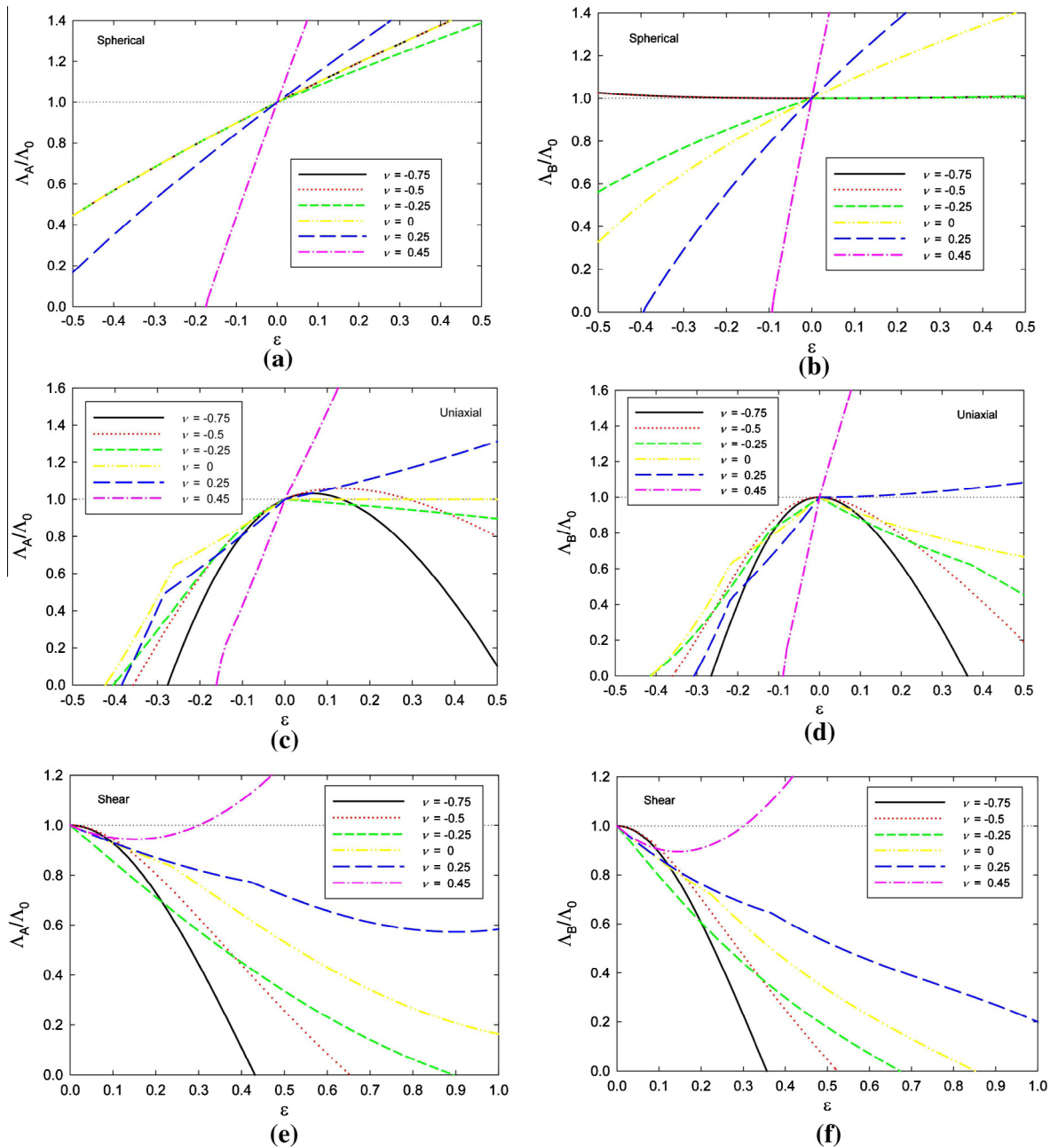


Fig. 1. Normalized minimum eigenvalues of stiffness tensors **A** and **B** for isotropic second-order elasticity ($C_{\alpha\beta\gamma}^0 = 0$): (a) spherical compression, **A** (b) spherical compression, **B** (c) uniaxial compression, **A** (d) uniaxial compression, **B** (e) shear, **A** (f) shear, **B**.

and various high pressure experiments suggest that the pressure derivative of the bulk modulus in the reference state obeys $2 < K' < 7$ for most such materials, with $3 < K' < 6$ typical (Steinberg, 1982; Jeanloz, 1989). Experimental data also suggest that the pressure derivative of the thermodynamic shear modulus in the reference state $1 < G' < 4$ for pure elements ((Guinan and Steinberg, 1974), correcting for G' differing from the definition in that reference by $G/3K + 1$). Also of high interest in the context of instability at high pressure are polycrystalline materials

with $G' < 0$ such as silicon carbide ($C'_{44} \approx -0.2$) (Clayton, 2010) and boron carbide ($-5 \lesssim C'_{44} \lesssim -2$) (Clayton, 2012). Means of constructing effective isotropic third-order constants for polycrystals from anisotropic single crystal constants are summarized in Mason and Maudlin (1999) and references therein.

In this work, third-order constants probing the domain $0 \leq K' \leq 10$ and $-10 \leq G' \leq 15$ are considered, as listed in Table 1. In the third-order elastic analysis, attention is restricted to $\nu = \frac{1}{4}$ (i.e., $\lambda = G = \frac{2}{3}K$), a sensible value

Table 1

Values of third-order elastic constants investigated for intrinsic stability.

Case	C_{111}^0	C_{112}^0	C_{123}^0	K'	G'
1	$0 \geq C_{111}^0 \geq -90K$	0	0	$0 \leq K' \leq 10$	$0 \leq G' \leq 15$
2	0	$0 \geq C_{112}^0 \geq -15K$	0	$0 \leq K' \leq 10$	0
3	0	0	$0 \geq C_{123}^0 \geq -45K$	$0 \leq K' \leq 10$	$-\frac{15}{2} \leq G' \leq 0$
4	$0 \geq C_{111}^0 \geq -10K$	$= C_{111}^0$	$= C_{111}^0$	$0 \leq K' \leq 10$	0
5	$40K \geq C_{111}^0 \geq -40K$	0	$= -\frac{1}{2}C_{111}^0$	0	$-10 \leq G' \leq 10$

representative of many metals, ceramics, and minerals. As discussed by Gilman (2003), $\nu = \frac{1}{4}$ (i.e., $C_{12}^0 = C_{44}^0$) is characteristic of the alkali metals and ionic crystals such as alkali halides that tend towards Cauchy symmetry. Covalently bonded materials, e.g., many ceramics, tend to have $\nu \leq \frac{1}{4}$, while engineering metals tend to have slightly larger ν , e.g., the mode is closer to $\frac{1}{3}$ for face centered cubic metals. Pure solid elements span the range $0.02 < \nu < 0.45$ (Gilman, 2003). Some values for particular materials are now quoted. Sodium chloride (alkali halide, rocksalt structure) and alumina (ceramic, trigonal structure) have $\nu \approx 0.24$ (Clayton, 2009). Two covalently bonded materials are silicon carbide ($\nu \approx 0.16$, hexagonal structure (Clayton, 2010)) and diamond ($\nu \approx 0.07$, cubic structure (McSkimin et al., 1972)). Most single crystals are anisotropic; values of ν mentioned thus far correspond to isotropic polycrystals. Two metals whose single crystals have low anisotropy are tungsten ($\nu \approx 0.28$, body centered cubic structure (Clayton, 2005)) and magnesium ($\nu \approx 0.27$, hexagonal structure (Clayton and Knap, 2011)). Concrete, essentially a porous mixture of minerals, has $\nu \approx 0.15$ (Clayton, 2008), though variations with composition are probable. In summary, $\nu = \frac{1}{4}$ is deemed a reasonable compromise of values mentioned above.

At fixed ν , it can be shown that energy W , stresses, and tangent elastic coefficients depend only on λ and $C_{\alpha\beta\gamma}^0/\lambda$, and Λ_0 depends only on λ (linearly). Hence Λ_C/Λ_0 , Λ_A/Λ_0 , and Λ_B/Λ_0 depend only on $C_{\alpha\beta\gamma}^0/\lambda$ and ε for a particular deformation path. For example, for Case 1 with $\nu = \frac{1}{4}$

$$\frac{W}{\lambda} = \frac{1}{2\lambda} \left(C_{IJKL}^0 + \frac{1}{3} C_{IJKLMN}^0 E_{MN} \right) E_{IJ} E_{KL},$$

$$\frac{1}{\lambda} C_{IJKL}^0 = \delta_{IJ} \delta_{KL} + \delta_{IK} \delta_{JL} + \delta_{IL} \delta_{JK},$$

$$\frac{1}{\lambda} C_{IJKLMN}^0 = \frac{1}{8} \frac{C_{111}^0}{\lambda} [\delta_{IK} (\delta_{JM} \delta_{LN} + \delta_{JN} \delta_{LM}) + \delta_{JL} (\delta_{IM} \delta_{KN} + \delta_{IN} \delta_{KM}) + \delta_{IL} (\delta_{JM} \delta_{KN} + \delta_{JN} \delta_{KM}) + \delta_{JK} (\delta_{IM} \delta_{LN} + \delta_{IN} \delta_{LM})],$$

where $0 \geq C_{111}^0/\lambda \geq -150$ in Table 1.

Shown in Fig. 2 are results for spherical deformation; in this deformation program stress is hydrostatic, i.e., $\sigma = -p\mathbf{1}$. Each subfigure shows minimum normalized eigenvalues of **C**, **A**, and **B** for two different sets of third-order elastic constants within prescribed domains for each of Cases 1–5 listed in Table 1. Recall that $\Lambda/\Lambda_0 = 1$ at $\varepsilon = 0$ for any stiffness matrix, and that $\Lambda/\Lambda_0 = 0$ at the onset of intrinsic instability as defined in the present work. Noteworthy observations are as follows:

- Case 1. [Fig. 2(a), $K' > 0$ and $G' > 0$] The material becomes increasingly stable (unstable) in compression (tension) with increasing K' and G' . The C, A, and B criteria give similar trends, with B more stringent in compression and C more stringent in tension.
- Case 2. [Fig. 2(b), $K' > 0$ and $G' = 0$] The material becomes increasingly unstable in compression with increasing K' . A change in critical eigenmode is observed in tension for $K' = 8.3$, leading to instability at $\varepsilon \geq 0.12$. The B criterion tends to be more stringent, especially in compression.
- Case 3. [Fig. 2(c), $K' > 0$ and $G' < 0$] The material becomes increasingly unstable in compression with decreasing G' . The B criterion tends to be more stringent, especially in compression.
- Case 4. [Fig. 2(d), $K' > 0$ and $G' = 0$] Results are identical to those for Case 2. This demonstrates the fact that for spherical loading of isotropic third-order elastic materials, internal stability depends only on K, G, K' , and G' , and not on all three independent third-order elastic constants considered individually.
- Case 5. [Fig. 2(e), $K' = 0$ and $G' > 0$ or $G' < 0$] The material becomes increasingly stable in compression (tension) with positive (negative) G' . The C, A, and B criteria give similar trends, with B more stringent in compression and C more stringent in tension.

Results in Fig. 2 confirm a particular example of a more general comparison theorem derived in Parry (1979) [Eq. (36) of that reference]; for a fixed material model, convexity with respect to stretch (i.e., A stability) is weaker than convexity with respect to Green strain (i.e., C stability) when $S_{11} = S_{22} = S_{33} = -J^{1/3}p \geq 0$.

Shown in Fig. 3 are results for uniaxial compression/tension; in this deformation program stress usually includes significant hydrostatic and deviatoric components. Noteworthy observations are as follows:

- Case 1. [Fig. 3(a), $K' > 0$ and $G' > 0$] The material becomes more unstable in tension with increasing K' and G' . The C, A, and B criteria give similar results for the critical strain at instability.
- Case 2. [Fig. 3(b), $K' > 0$ and $G' = 0$] The material becomes increasingly unstable in compression and tension with increasing K' . The B criterion tends to be more stringent, especially in compression.

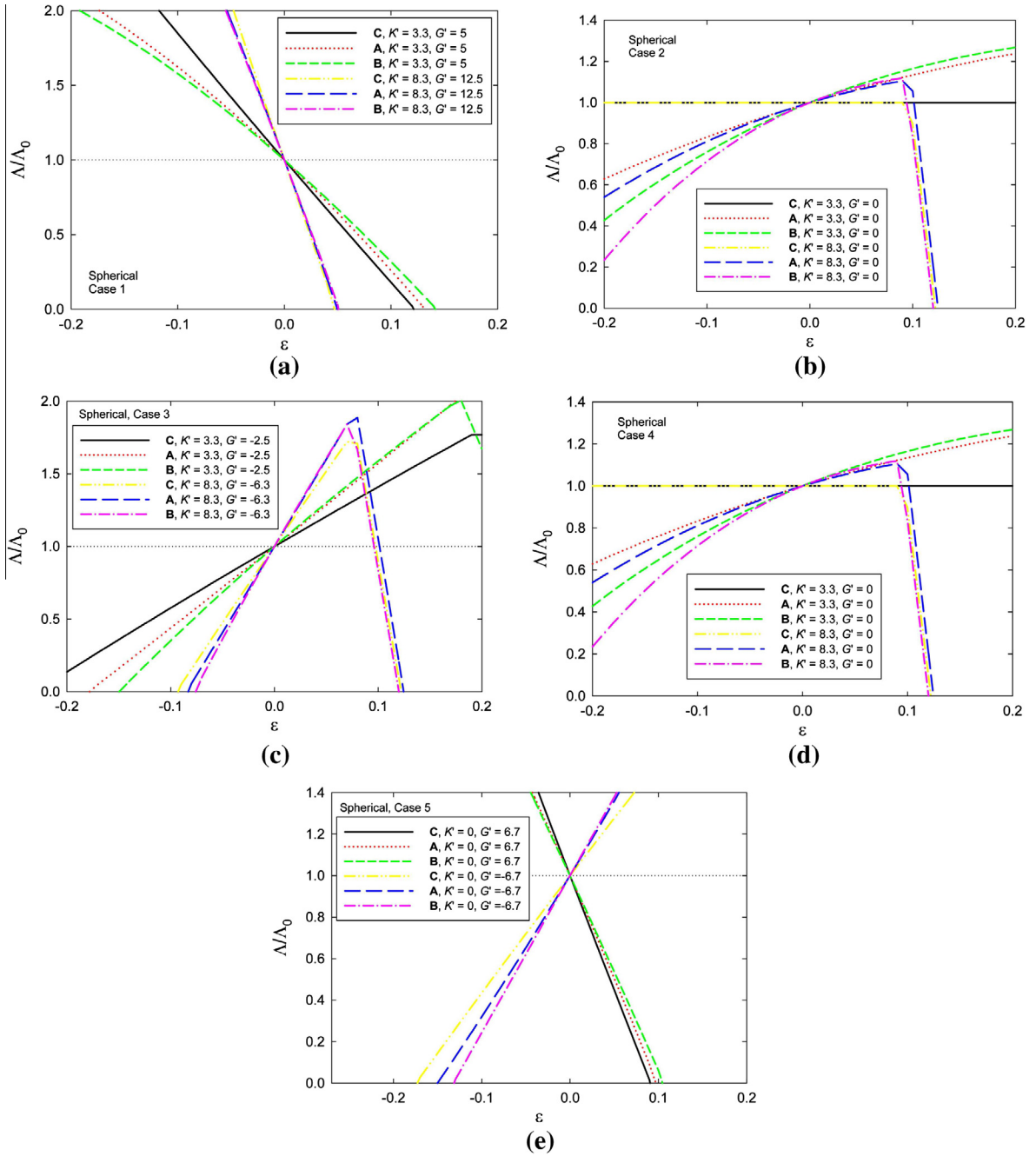


Fig. 2. Normalized minimum eigenvalues of stiffness tensors **C**, **A**, and **B** for isotropic third-order elasticity and spherical deformation: (a) case 1, $C_{111}^0 \neq 0$ (b) case 2, $C_{112}^0 \neq 0$ (c) case 3, $C_{123}^0 \neq 0$ (d) case 4, $C_{111}^0 = C_{112}^0 = C_{123}^0 \neq 0$ (e) case 5, $C_{111}^0 = -2C_{123}^0 \neq 0$.

Case 3. [Fig. 3(c), $K' > 0$ and $G' < 0$] The material becomes increasingly unstable in compression and tension with decreasing G' . The domain of intrinsic stability is small for $G' = -6.3$, i.e. $-0.03 \lesssim \epsilon \lesssim 0.05$. The C, A, and B criteria give similar results in compression.

Case 4. [Fig. 3(d), $K' > 0$ and $G' = 0$] Unlike what was observed for spherical deformation, results for uniaxial strain differ from those in Case 2.

However, like Case 2, the material becomes increasingly unstable in compression and tension with increasing K' .

Case 5. [Fig. 3(e), $K' = 0$ and $G' > 0$ or $G' < 0$] The domain of intrinsic stability shifts towards compression (tension) with positive (negative) G' . The C, A, and B criteria give similar trends, with B more stringent in compression and C more stringent in tension.

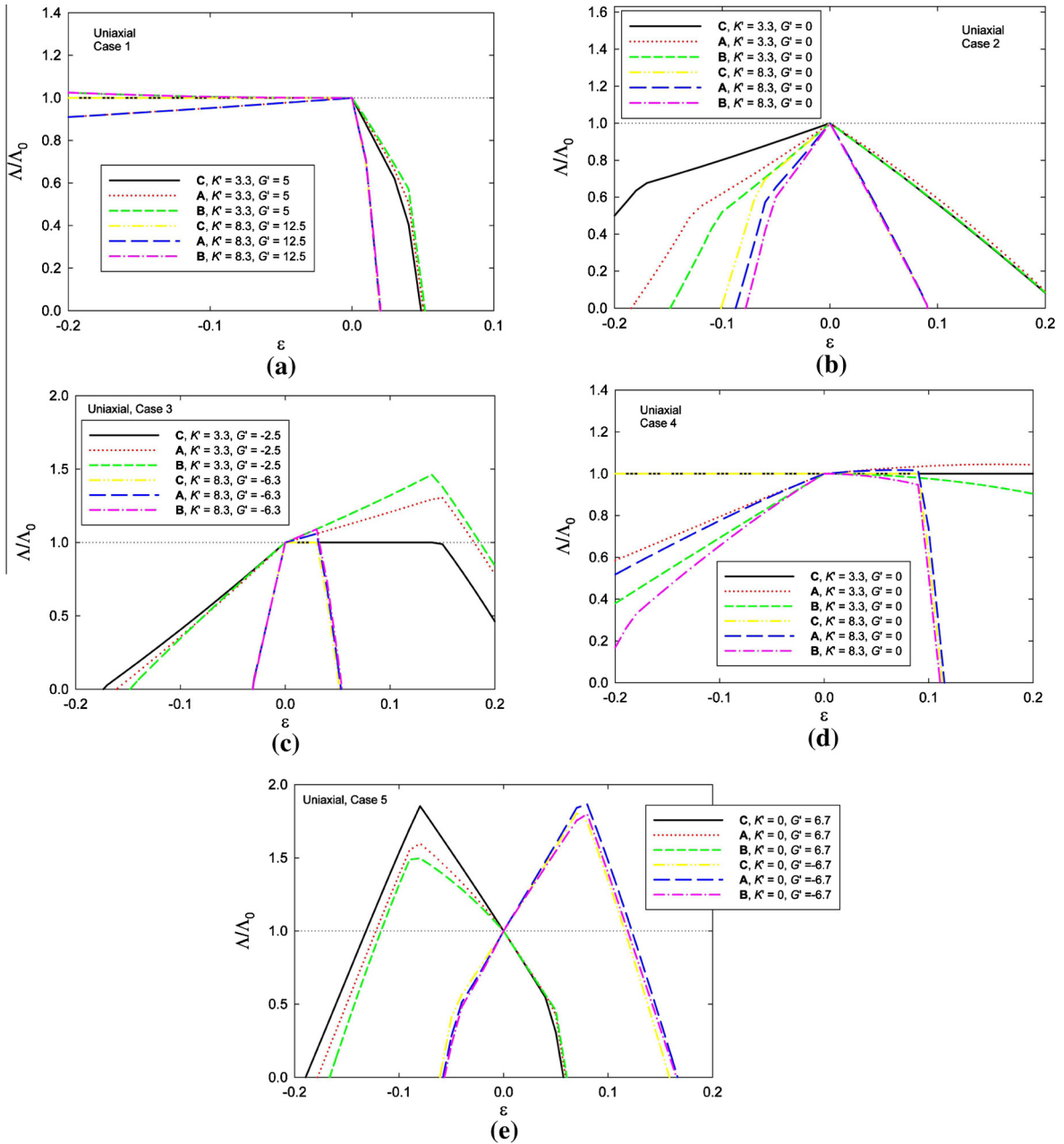


Fig. 3. Normalized minimum eigenvalues of stiffness tensors C, A, and B for isotropic third-order elasticity and uniaxial strain: (a) case 1, $C_{111}^0 \neq 0$ (b) case 2, $C_{112}^0 \neq 0$ (c) case 3, $C_{123}^0 \neq 0$ (d) case 4, $C_{111}^0 = C_{112}^0 = C_{123}^0 \neq 0$ (e) case 5, $C_{111}^0 = -2C_{123}^0 \neq 0$.

Shown in Fig. 4 are results for simple shear; in this deformation program stress includes comparatively large deviatoric components, though hydrostatic stress does not generally vanish due to geometric nonlinearity, i.e., Kelvin and Poynting effects (Eringen, 1962), and may be large as a result of large strain or large material nonlinearity. Noteworthy observations are as follows:

Case 1. [Fig. 4(a), $K' > 0$ and $G' > 0$] The material becomes more unstable at large shear with

increasing K' and G' . The C, A, and B criteria give similar results for the critical strain at instability.

Case 2. [Fig. 4(b), $K' > 0$ and $G' = 0$] The material becomes increasingly unstable in shear with increasing K' . The B criterion is the most stringent.

Case 3. [Fig. 4(c), $K' > 0$ and $G' < 0$] The material becomes increasingly unstable in shear with decreasing G' . The C, A, and B criteria give similar results, with C most stringent.

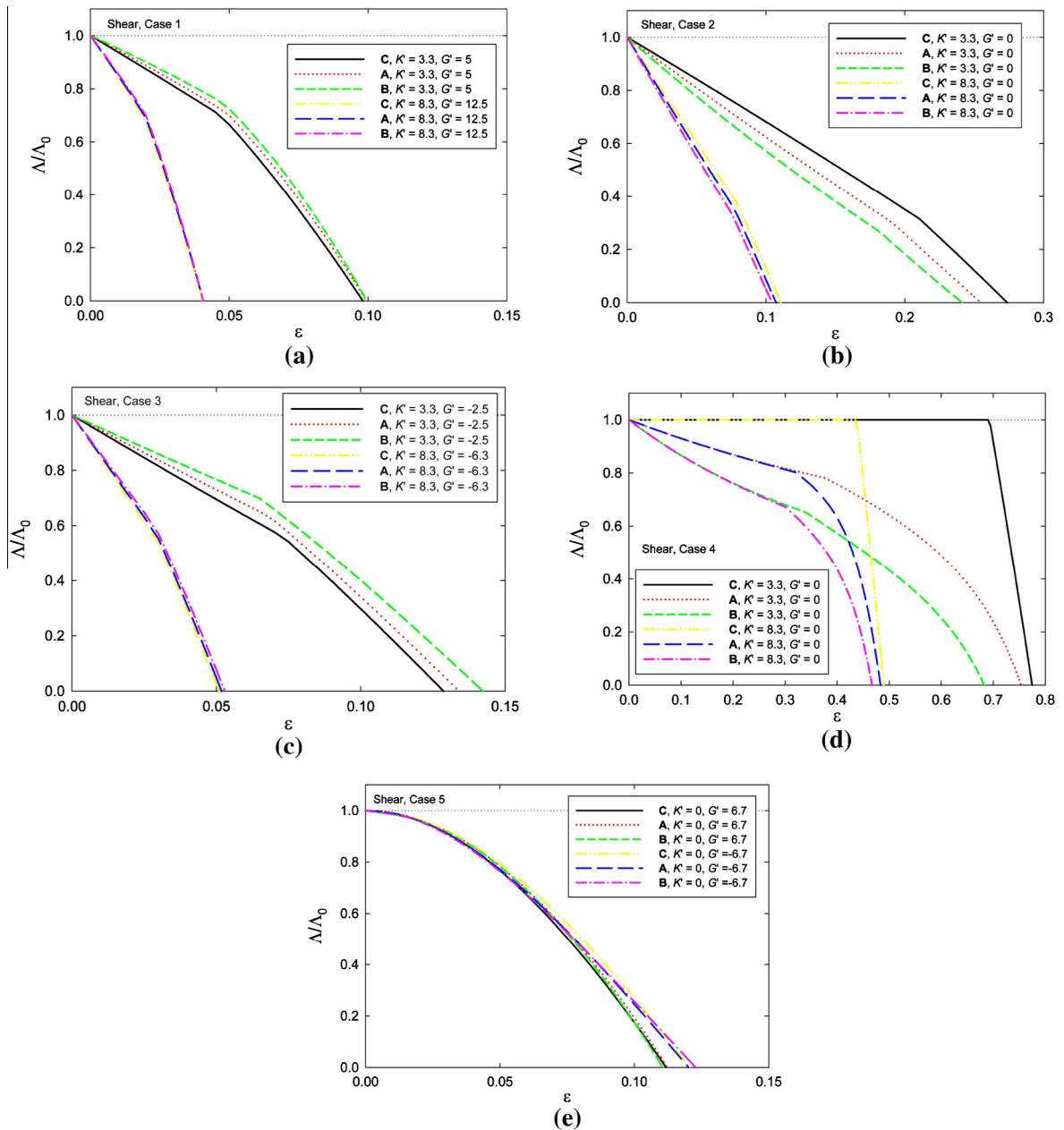


Fig. 4. Normalized minimum eigenvalues of stiffness tensors **C**, **A**, and **B** for isotropic third-order elasticity and shear deformation: (a) case 1, $C_{111}^0 \neq 0$ (b) case 2, $C_{112}^0 \neq 0$ (c) case 3, $C_{123}^0 \neq 0$ (d) case 4, $C_{111}^0 = C_{112}^0 = C_{123}^0 \neq 0$ (e) case 5, $C_{111}^0 = -2C_{123}^0 \neq 0$.

- Case 4. [Fig. 4d, $K' > 0$ and $G' = 0$] Unlike what was observed for spherical deformation, results for simple shear differ from those in Case 2. The material becomes increasingly unstable with increasing K' , but very large strains ($\epsilon > 0.45$) are attained prior to instability.
- Case 5. [Fig. 4(e), $K' = 0$ and $G' > 0$ or $G' < 0$] Comparison with Fig. 1(e) and 1(f) demonstrates that the material becomes increasingly unstable with increasing magnitude of G' , regardless of sign of G' . The case with $G' < 0$ has a slightly

larger critical strain ($\epsilon^* \approx 0.12$) than the case with $G' > 0$ ($\epsilon^* \approx 0.11$). The C, A, and B criteria give similar predictions for the minimum eigenvalue.

By inspection, Λ_C does not depend on rotation \mathbf{R} entering (3.4). For results presented in this paper, it was also found that critical strain ϵ^* at instability corresponding to $\Lambda_A = 0$ or $\Lambda_B = 0$ did not change if stretch \mathbf{U} was prescribed rather than $\mathbf{R}\mathbf{U}$ in (3.4); i.e., rigid rotation did not affect loss of internal stability in simple shear. Specifically, Λ_B does not depend at all on rotation R since **B** is an

objective fourth order tensor, and while Λ_A can depend on R , such dependence was found to be inconsequential at applied shear strains up to the onset of internal instability.

3.3. Neo-Hookean elasticity

In the reference state, $C_{ijkl} = C_{ijkl}^0$ and internal stability conditions are again the familiar constraints

$$\det[C_{\alpha\beta}^0] > 0 \iff \Lambda_0 > 0 \iff K > 0 \text{ and } G > 0. \quad (3.6)$$

The rightmost conditions in (3.6) again imply $-1 < \nu < \frac{1}{2}$. Noting that $G = \lambda(\frac{1}{2\nu} - 1)$, at a given value of ν , it follows that strain energy W , stresses, and tangent elastic coefficients are all proportional to λ . Hence Λ_C/Λ_0 , Λ_A/Λ_0 , and Λ_B/Λ_0 depend only on ν and ε for a particular prescribed deformation path. Considered in Fig. 5 are results for $-1 < \nu < \frac{1}{2}$. These results are analogous to those of Fig. 1, but with a compressible neo-Hookean model rather than a second-order Green elasticity model.

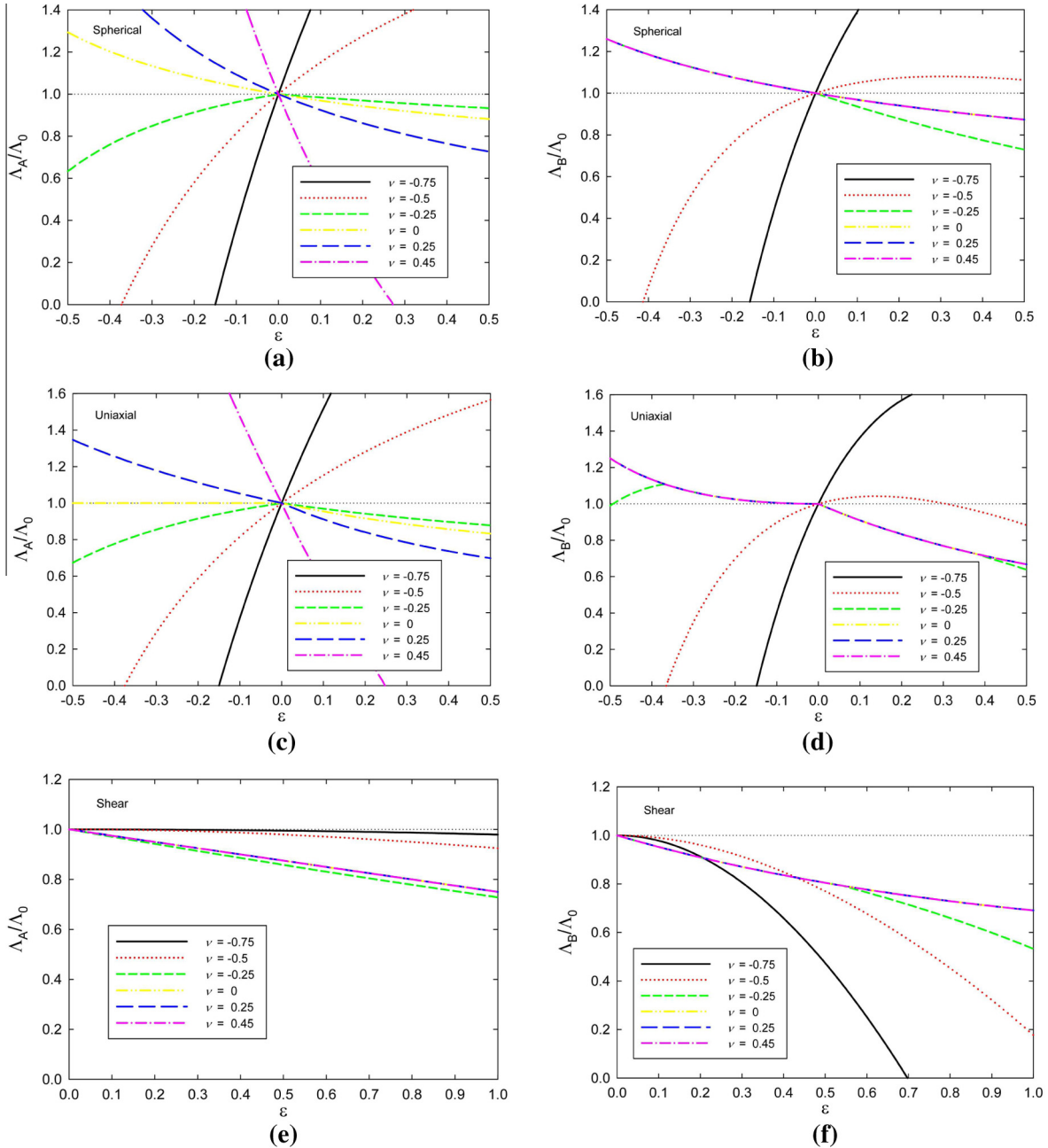


Fig. 5. Normalized minimum eigenvalues of stiffness tensors **A** and **B** for neo-Hookean elasticity: (a) spherical compression, **A** (b) spherical compression, **B** (c) uniaxial compression, **A** (d) uniaxial compression, **B** (e) shear, **A** (f) shear, **B**.

As shown in Fig. 5(a) and (b) for spherical deformation, as ν increases, stability in tension ($\varepsilon > 0$) decreases, and in compression ($\varepsilon < 0$) increases. The A and B stability criteria of (2.17) and (2.26) yield notably different results. For non-negative ν , comparison with Fig. 1(a) and (b) shows that the neo-Hookean material tends to be much more stable in compression than the second-order elastic solid. As shown in Fig. 5(c) and (d) for uniaxial strain, for $-0.25 \leq \nu \leq 0.25$, the material remains intrinsically stable over the large domain of strain studied ($-0.5 \leq \varepsilon \leq 0.5$), though the A [Fig. 5(c)] and B [Fig. 5(d)] criteria provide different results. As shown in Fig. 5(e) and (f) for simple shear, Λ_A and Λ_B remain positive for $\nu \geq -0.5$ and $\varepsilon \leq 1.0$. Trends for Λ_C are qualitatively similar to those for Λ_A and Λ_B and are shown in Fig. 6 for $\nu = \frac{1}{4}$.

3.4. Summary and discussion of critical eigenmodes

Critical strain ε^* and corresponding eigenmode components δe_x^* at the onset of B instability ($\Lambda_B = 0$ at ε^*) are listed in Table 2 for representative cases considered in Section 3.3. Results are given for $\nu = \frac{1}{4}$. The B stability criterion is presumably of highest interest since results in Section 3.3 demonstrated it to be equally or more stringent than C or A criteria for compressive and shear loading paths, for most values of elastic constants considered.

For spherical or uniaxial loading, (+) denotes tension with $\varepsilon^* > 0$, and (–) denotes compression with $\varepsilon^* < 0$. Absent rows denote that a zero eigenvalue is not attained for that case. Extra rows for a particular case denote a duplicate null eigenvalue and its corresponding critical eigenmode, one for each multiplicity of zero eigenvalue. Recall that an eigenmode with $\delta e_1^* = \delta e_2^* = \delta e_3^* \neq 0$ and $\delta e_4^* = \delta e_5^* = \delta e_6^* = 0$ corresponds to a volumetric instability; conversely, an eigenmode with $\delta e_1^* + \delta e_2^* + \delta e_3^* = 0$ corresponds to a shear instability. An intrinsic volumetric instability is associated with a degenerate incremental bulk modulus, and in a real material might signify cavitation (Wang et al., 1993; Wang et al., 1995) or mode I fracture. An intrinsic shear instability is associated with a degenerate incremental shear modulus, and in a real material might signify localized slip, twinning (Rosakis and Tsai,

1994), or mode II/III fracture. An eigenmode that is neither purely volumetric nor pure shear is referred to as a mixed instability. The following observations from Table 2 regarding internal instabilities are noteworthy:

Second-order elasticity. Instability under spherical compression corresponds to five simultaneous shearing modes. Instabilities under uniaxial compression and simple shear are mixed.

Third-order elasticity, Case 1. Instability under spherical extension corresponds to five simultaneous shearing modes. Instabilities under uniaxial extension and simple shear are mixed.

Third-order elasticity, Case 2. Instability under spherical extension is volumetric. Instability under spherical compression corresponds to five simultaneous shearing modes. Instability under uniaxial extension is a shearing mode. Instabilities under simple shear and uniaxial compression are mixed.

Third-order elasticity, Case 3. Instability under spherical extension is volumetric. Instability under spherical compression corresponds to five simultaneous shearing modes. Instability under uniaxial extension is mixed. Instability under uniaxial compression corresponds to two simultaneous shearing modes. Instability under simple shear is mixed.

Third-order elasticity, Case 4. Instability under spherical extension is volumetric. Instability under spherical compression corresponds to five simultaneous shearing modes. Instability under uniaxial extension, uniaxial compression, and simple shear are mixed.

Third-order elasticity, Case 5. Instability under spherical compression corresponds to five simultaneous shearing modes. Instabilities under uniaxial extension, uniaxial compression, and simple shear are mixed.

Neo-Hookean elasticity. No intrinsic instabilities are observed or even approached for spherical loading ($|\varepsilon| \leq 0.8$), uniaxial loading ($|\varepsilon| \leq 0.8$), or simple shear loading ($\varepsilon \leq 1$) for $\nu = \frac{1}{4}$; therefore, $|\varepsilon^*| \gg 0.8$.

Cases 2, 3, and 4 demonstrate volumetric intrinsic stabilities in hydrostatic extension which are coaxial with the prescribed primary deformation path. All other instabilities occur in directions that differ from the direction of primary loading, meaning virtual strain increments are not

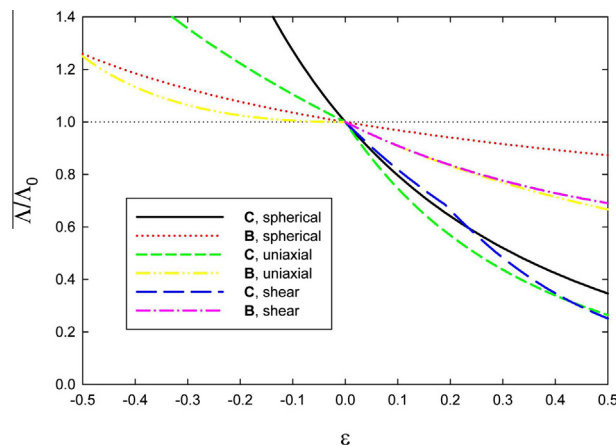


Fig. 6. Normalized minimum eigenvalues of stiffness tensors C and B for neo-Hookean elasticity with $\nu = \frac{1}{4}$.

Table 2

Critical ε^* (positive in tension or shear) and corresponding eigenmodes δe_x^* for B instability, $\nu = \frac{1}{4}$

Model (Case)	K'	G'	Loading	ε^*	δe_1^*	δe_2^*	δe_3^*	δe_4^*	δe_5^*	δe_6^*	
Second-order	0	0	spherical (-)	-0.40	0.21	-0.79	0.58	0	0	0	
					-0.79	0.21	0.58	0	0	0	
					0	0	0	1	0	0	
					0	0	0	0	1	0	
					0	0	0	0	0	1	
Third-order (1) ($C_{111}^0/\lambda = -150$)	10	15	uniaxial (-) shear	-0.31 1.2	0.96	-0.19	-0.19	0	0	0	
					0.27	0.68	0.047	0	0	-0.68	
					0.042	0.21	-0.79	0.58	0	0	0
					-0.79	0.21	0.58	0	0	0	
					0	0	0	1	0	0	
Third-order (2) ($C_{112}^0/\lambda = -25$)	10	0	spherical (+) spherical (-)	0.10 -0.22	0.58	0.58	0.58	0	0	0	
					0.41	0.41	-0.82	0	0	0	
					0.71	-0.71	0	0	0	0	
					0	0	0	1	0	0	
					0	0	0	0	0	1	
Third-order (3) ($C_{123}^0/\lambda = -75$)	10	$-\frac{15}{2}$	uniaxial (+) uniaxial (-) shear	0.077 -0.067 0.088	0	0.71	-0.71	0	0	0	
					-0.85	0.37	0.37	0	0	0	
					-0.25	-0.28	0.46	0	0	0.80	
					0.10	0.58	0.58	0.58	0	0	0
					-0.067	-0.27	-0.53	0.80	0	0	0
Third-order (4) ($C_{111}^0/\lambda = -50/3$)	10	0	spherical (+) spherical (-)	0.10 -0.22	-0.77	0.62	0.15	0	0	0	
					0	0	0	1	0	0	
					0	0	0	0	1	0	
					0	0	0	0	0	1	
					0	0	0	0	0	1	
Third-order (5) ($C_{111}^0/\lambda = +200/3$)	0	-10	uniaxial (+) uniaxial (-) shear	0.094 -0.21 0.43	-0.35	0.66	0.66	0	0	0	
					0	0.71	-0.71	0	0	0	
					0	0	0	1	0	0	
					0.11	0.092	-0.53	0	0	0.84	
					0.10	0.58	0.58	0.58	0	0	0
Third-order (6) ($C_{111}^0/\lambda = -50/3$)	10	0	spherical (+) spherical (-)	0.10 -0.22	0.71	-0.71	0	0	0	0	
					0.41	0.41	-0.82	0	0	0	
					0	0	0	1	0	0	
					0	0	0	0	1	0	
					0	0	0	0	0	1	
Third-order (7) ($C_{111}^0/\lambda = +200/3$)	0	-10	uniaxial (+) uniaxial (-) shear	0.11 -0.038 0.080	-0.053	0.71	0.71	0	0	0	
					0.97	-0.18	-0.18	0	0	0	
					0.080	0.26	0.29	0.22	0	0	-0.89
					-0.054	-0.81	0.47	0.34	0	0	0
					0.078	0.67	-0.74	0	0	0	
Neo-Hookean	$\frac{26}{15}$	$\frac{7}{5}$	any	≥ 0.8							

aligned with prescribed deformations of Section 3.1. In a real material, a local strain perturbation due to a defect in the material might be sufficient to trigger a localization or failure mode in such a direction, presuming any constraints imposed by the environment permit such phenomena.

Apparent trends in intrinsic stability of isotropic solids under primary deformation paths of spherical compression, uniaxial strain compression, and simple shear have been deduced in this work. These are perhaps the simplest fundamental deformation-controlled loading paths, and

correlate with real experiments such as diamond anvil cell compression, shock compression, and direct shear loading, respectively. Other fundamental loading protocols not studied here include uniaxial stress (Morris and Krenn, 2000) and all-around dead loading (Rivlin, 1974), which have been analyzed elsewhere, but not for third-order Green elastic and compressible neo-Hookean models studied in the present work. Results cannot, in general, be immediately translated to other loading paths possible in generic applications. As demonstrated by Parry (1980), no universally weakest stability criterion exists. For a fixed

Table 3Eigenvalue ratios, B stability, spherical and uniaxial compression, $\nu \geq 0.4$.

	Spherical, $\varepsilon = -0.05$	Spherical, $\varepsilon = -0.10$	Uniaxial, $\varepsilon = -0.05$	Uniaxial, $\varepsilon = -0.10$
$(\Lambda_B/\Lambda_0)_{\nu=0.4}$	0.7437	0.4737	0.7084	0.4324
r_1^B	-4.2079	-18.0217	-4.2040	-18.7845
r_2^B	15.7529	12.1098	16.4888	12.6963
r_3^B	10.3652	10.1742	10.4046	10.2124
r_4^B	10.0352	10.0171	10.0389	10.0208
r_5^B	10.0035	10.0017	10.0039	10.0021
r_6^B	10.0004	10.0002	10.0004	10.0002
r_7^B	10.0000	10.0000	10.0000	10.0000

material, the most stringent criterion for stability depends on the loading mode. For a fixed loading mode, the most stringent criterion depends on material properties. Comparison theorems among different criteria that depend on different Lagrangian coordinates have been derived (Parry, 1978; Parry, 1979); as noted already in the text describing Fig. 2, one such theorem agrees with the present analysis of C and A criteria for third-order elastic bodies under hydrostatic tension.

4. Conclusions

Intrinsic stability of several kinds of nonlinear elastic isotropic solids has been analyzed for homogeneous deformation paths, specifically spherical extension–compression, uniaxial tension–compression, and simple shear. Loss of internal stability according to the C, A, or B criterion corresponds to first appearance of a null eigenvalue of an incremental stiffness matrix associated with second Piola–Kirchhoff, first Piola–Kirchhoff, or Cauchy stress, respectively. Effects of choices of second- and third-order elastic constants on stability have systematically studied for second- and third-order Green elastic solids and compressible neo-Hookean solids. For most cases investigated here, especially those involving compression, intrinsic stability according to increments in Cauchy stress (i.e., B criterion) is found to be the most stringent. When third-order constants vanish (i.e., a St. Venant–Kirchhoff solid), intrinsic stability under large compression tends to decrease as Poisson's ratio increases. When third-order constants are nonzero, a negative (positive) pressure derivative of the shear modulus often leads to unstable modes in compression (tension). When pressure derivatives of bulk and shear moduli are equal, but particular third-order elastic constants differ, internal stability is the same for spherical deformation but may differ for uniaxial tension/compression. For simple shear, larger magnitudes of third-order constants promote less stable behavior, regardless of the sign of the pressure derivative of the shear modulus. A compressible neo-Hookean elastic model demonstrates greater intrinsic stability than the third-order elastic model when Poisson's ratio is non-negative.

Appendix A. Minimum eigenvalue ratios in the limit of incompressibility

As Poisson's ratio $\nu \rightarrow \frac{1}{2}$, an isotropic solid approaches incompressibility. Consider a Green elastic material of the

type described in Section 2.2, with vanishing third-order elastic constants. At a fixed strain state, define ratios of minimum eigenvalues as Poisson's ratio is varied by the series

$$r_1^X = \frac{\Lambda_X|_{\nu=0.49}}{\Lambda_X|_{\nu=0.4}}, \quad r_2^X = \frac{\Lambda_X|_{\nu=0.499}}{\Lambda_X|_{\nu=0.49}}, \dots, \quad r_k^X = \frac{\Lambda_X|_{\nu=0.5-10^{-(k+1)}}}{\Lambda_X|_{\nu=0.5-10^{-k}}}, \dots \quad (\text{A.1})$$

Here, X can refer to the minimum eigenvalue of stiffness matrix A or B, and k is a positive integer. Calculations show that $r_k^X \rightarrow 10$ with increasing k for any of the deformation paths and values of imposed strain ε considered in Section 3, and for both X = A and X = B. Representative results are listed in Table 3 for spherical and uniaxial compression and X = B, demonstrating how rapidly intrinsic stability is compromised in compression as the material loses compressibility. In other words, since $r_1^B < 0$, minimum eigenvalues become strongly negative as k increases.

References

- Born, M., 1940. On the stability of crystal lattices. I. Math. Proc. Camb. Philos. Soc. 36, 160–172.
- Chen, M., McCauley, J., Hemker, K., 2003. Shock-induced localized amorphization in boron carbide. Science 299, 1563–1566.
- Clayton, J., 2005. Dynamic plasticity and fracture in high density polycrystals: constitutive modeling and numerical simulation. J. Mech. Phys. Solids 53, 261–301.
- Clayton, J., 2006. Continuum multiscale modeling of finite deformation plasticity and anisotropic damage in polycrystals. Theor. Appl. Fract. Mech. 45, 163–185.
- Clayton, J., 2008. A model for deformation and fragmentation in crushable brittle solids. Int. J. Impact Eng. 35, 269–289.
- Clayton, J., 2009. A continuum description of nonlinear elasticity, slip and twinning, with application to sapphire. Proc. R. Soc. Lond. A 465, 307–334.
- Clayton, J., 2010. Modeling nonlinear electromechanical behavior of shocked silicon carbide. J. Appl. Phys. 107, 013520.
- Clayton, J., 2011. Nonlinear Mechanics of Crystals. Springer, Dordrecht.
- Clayton, J., 2012. Towards a nonlinear elastic representation of finite compression and instability of boron carbide ceramic. Philos. Mag. 92, 2860–2893.
- Clayton, J., 2012. On anholonomic deformation, geometry, and differentiation. Math. Mech. Solids 17, 702–735.
- Clayton, J., Knap, J., 2011. A phase field model of deformation twinning: nonlinear theory and numerical simulation. Physica D 240, 841–858.
- Clayton, J., McDowell, D., 2004. Homogenized finite elastoplasticity and damage: theory and computations. Mech. Mater. 36, 799–824.
- Eringen, A., 1962. Nonlinear Theory of Continuous Media. McGraw-Hill, New York.
- Fuller, T., Brannon, R., 2011. On the thermodynamic requirement of elastic stiffness anisotropy in isotropic materials. Int. J. Eng. Sci 49, 311–321.
- Gilman, J., 2003. Electronic Basis of the Strength of Materials. Cambridge Univ. Press, Cambridge.
- Gregoryanz, E., Hemley, R., Mao, H., Gillet, P., 2000. High-pressure elasticity of α -quartz: instability and ferroelastic transition. Phys. Rev. Lett. 84, 3117–3120.

- Guinan, M., Steinberg, D., 1974. Pressure and temperature derivatives of the isotropic polycrystalline shear modulus for 65 elements. *J. Phys. Chem. Solids* 35, 1501–1512.
- Hill, R., 1957. On uniqueness and stability in the theory of finite elastic strain. *J. Mech. Phys. Solids* 5, 229–241.
- Hill, R., 1975. On the elasticity and stability of perfect crystals at finite strain. *Math. Proc. Camb. Phil. Soc.* 77, 225–240.
- Hill, R., Milstein, F., 1977. Principles of stability analysis of ideal crystals. *Phys. Rev. B* 15, 3087–3096.
- Jeanloz, R., 1989. Shock wave equation of state and finite strain theory. *J. Geophys. Res.* 94, 5873–5886.
- Mason, T., Maudlin, P., 1999. Effects of higher-order anisotropic elasticity using textured polycrystals in three-dimensional wave propagation problems. *Mech. Mater.* 31, 861–882.
- McSkimin, H., Andreatch, P., Glynn, P., 1972. The elastic stiffness moduli of diamond. *J. Appl. Phys.* 43, 985–987.
- Milstein, F., Hill, R., 1979. Divergences among the born and classical stability criteria for cubic crystals under hydrostatic loading. *Phys. Rev. Lett.* 43, 1411–1413.
- Milstein, F., Hill, R., 1979. Theoretical properties of cubic crystals at arbitrary pressure –III. Stability. *J. Mech. Phys. Solids* 27, 255–279.
- Misra, R., 1940. On the stability of crystal lattices. II. *Math. Proc. Camb. Philos. Soc.* 36, 173–182.
- Morris, J., Krenn, C., 2000. The internal stability of an elastic solid. *Philos. Mag. A* 80, 2827–2840.
- Murnaghan, F., 1937. Finite deformations of an elastic solid. *Am. J. Math.* 59, 235–260.
- Parry, G., 1978. On the relative strengths of intrinsic stability criteria. *Q. J. Mech. Appl. Math.* 31, 1–7.
- Parry, G., 1979. On the comparison of stability criteria in anisotropic materials. *Math. Proc. Camb. Philos. Soc.* 86, 529–538.
- Parry, G., 1980. On the relative strengths of stability criteria in anisotropic materials. *Mech. Res. Commun.* 7, 93–98.
- Rashid, M., Nemat-Nasser, S., 1992. A constitutive algorithm for rate-dependent crystal plasticity. *Comput. Methods Appl. Mech. Eng.* 94, 201–228.
- Rivlin, R., 1974. Stability of pure homogeneous deformations of an elastic cube under dead loading. *Q. Appl. Math.* 32, 265–271.
- Rivlin, R., Beatty, M., 2003. Dead loading of a unit cube of compressible isotropic material. *Z. Angew. Math. Phys.* 54, 954–963.
- Rosakis, P., Tsai, H., 1994. On the role of shear instability in the modelling of crystal twinning. *Mech. Mater.* 17, 245–259.
- Simo, J., Pister, K., 1984. Remarks on rate constitutive equations for finite deformation problems: computational implications. *Comput. Methods Appl. Mech. Eng.* 46, 201–215.
- Steinberg, D., 1982. Some observations regarding the pressure dependence of the bulk modulus. *J. Phys. Chem. Solids* 43, 1173–1175.
- Teodosiu, C., 1982. *Elastic Models of Crystal Defects*. Springer-Verlag, Berlin.
- Thurston, R., 1974. Waves in Solids. In: Truesdell, C. (Ed.), *Handbuch der Physik* VIA/4. Springer-Verlag, Berlin, pp. 109–308.
- Thurston, R., McSkimin, H., Andreatch, P., 1966. Third-order elastic coefficients of quartz. *J. Appl. Phys.* 37, 267–275.
- Wallace, D., 1967. Thermoelasticity of stressed materials and comparison of various elastic constants. *Phys. Rev.* 162, 776–789.
- Wallace, D., 1972. *Thermodynamics of Crystals*. John Wiley & Sons, New York.
- Wang, C.-C., Truesdell, C., 1973. *Introduction to Rational Elasticity*. Noordhoff, Leyden.
- Wang, J., Yip, S., Phillpot, S., Wolf, D., 1993. Crystal instabilities at finite strain. *Phys. Rev. Lett.* 71, 4182–4185.
- Wang, J., Li, J., Yip, S., Phillpot, S., Wolf, D., 1995. Mechanical instabilities of homogeneous crystals. *Phys. Rev. B* 52, 627–635.
- Weaver, J., 1976. Application of finite strain theory to non-cubic crystals. *J. Phys. Chem. Solids* 37, 711–718.

<u>NO. OF</u> <u>COPIES</u>	<u>ORGANIZATION</u>
1 (PDF)	DEFENSE TECHNICAL INFORMATION CTR DTIC OCA
1 (PDF)	DIRECTOR US ARMY RESEARCH LAB IMAL HRA
1 (PDF)	DIRECTOR US ARMY RESEARCH LAB RDRL CIO LL
1 (PDF)	GOVT PRINTG OFC A MALHOTRA
35 (PDF)	DIR USARL RDRL CI P PLOSTINS RDRL CIH C J KNAP RDRL WM R DONEY B FORCH J MCCAULEY RDRL WML B I BATYREV B RICE D TAYLOR N WEINGARTEN RDRL WML H B SCHUSTER RDRL WMM J BEATTY RDRL WMM B G GAZONAS C RANDOW T SANO RDRL WMM E J SWAB RDRL WMM F M TSCHOPP RDRL WMM G J ANDZELM RDRL WMP S SCHOENFELD RDRL WMP B C HOPPEL D POWELL S SATAPATHY M SCHEIDLER T WEERASOORIYA

<u>NO. OF</u> <u>COPIES</u>	<u>ORGANIZATION</u>
	RDRL WMP C R BECKER S BILYK T BJERKE D CASEM J CLAYTON D DANDEKAR M GREENFIELD R LEAVY J LLOYD M RAFTENBERG S SEGLETES C WILLIAMS

INTENTIONALLY LEFT BLANK.